phys. stat. sol. (a) **205**, No. 7, 1666–1671 (2008) / **DOI** 10.1002/pssa.200723629

physica status solidi a
www.pss-a.com
applications and materials science

Nonlinear-laser $\chi^{(3)}$- and $\chi^{(2)}$-effects in fine-grained highly transparent optical $Ba(Mg,Zr,Ta)O_3$ ceramics and their microhardness

A. A. Kaminskii[*,1], M. Sh. Akchurin[1], N. Tanaka[2], H. J. Eichler[3], H. Rhee[3], K. Ueda[4], K. Takaichi[4], A. Shirakawa[4], M. Tokurakawa[4], J. Dong[,4], Y. Kintaka[2], S. Kuretake[2], and Y. Sakabe[2]**

[1] Institute of Crystallography, Russian Academy of Sciences, Moscow 119333, Russia
[2] Murata Manufacturing Co., Ltd., 1-10-1 Higashi-kotari, Nagaokakyo-shi, Kyoto, Japan
[3] Institute of Optics and Atomic Physics, Technical University of Berlin, Berlin 10623, Germany
[4] Institute for Laser Science, University of Electro-Communications, Tokyo 182-8585, Japan

Received 9 December 2007, revised 15 February 2008, accepted 27 February 2008
Published online 28 May 2008

PACS 42.55.Rz, 42.65.Dr, 42.65.Ky, 78.30.Hv

[*] Corresponding author: e-mail kaminalex@mail.ru
[**] Present address: Department of Physics, School of Engineering and Physical Science, Heriot-Watt University, Edinburgh EH144AS, United Kingdom

We report on laser-induced $\chi^{(3)}$- and $\chi^{(2)}$-nonlinear generation in novel optical ceramics, $Ba(Mg,Zr,Ta)O_3$, with "disordered" O_h^5-cubic structure, namely high-order Stokes and anti-Stokes lasing, third- and second-harmonic generation under one-micrometer picosecond pumping. Microhardness and fracture toughness were also measured.

1 Introduction In the last decade solid-state gain materials for laser physics and their applications are increasingly employed in the crystalline ceramic form [1]. With these novel materials very impressive laser advances have already been made, e.g. the achievement with laser-diode pumping of about 100 kW output CW power of O_h^{10}-garnet structure ceramics of $Nd^{3+}:Y_3Al_5O_{12}$ laser [2] ($^4F_{3/2} \rightarrow {}^4I_{11/2}$ generation intermanifold transition) and efficient sub-50 fs one-micrometer ytterbium ceramic lasers ($^2F_{5/2} \rightarrow {}^2F_{7/2}$) on the base of rare-earth sesquioxides with the T_h^7-bixbyite structure [3]). Recently, it was found that the grain boundaries in these Konoshima Co. ceramics improved mechanical toughness and microhardness to the same laser-host crystals (see, e.g. [4]). Another Japanese company (Murata Manufacturing) recently developed a highly transparent ceramics ("Lumicera type-Z") for high-refractive optical lenses [5], offering "disordered" perovskite O_h^5-structure. They are also promising host materials for trivalent lanthanide (Ln^{3+}) and transition-metal (TM) lasants. The walls of nano- or micro-size grains of all the above-mentioned ceramics are surface defects where the centrosymmetric cubic crystallographic nature is broken. Therefore, in these bulk ceramic materials having high concentration of grain-boundary walls both cubic $\chi^{(3)}$- and quadratic $\chi^{(2)}$-nonlinearities should be manifested under high peak power of laser excitation, namely stimulated Raman scattering (SRS), low intensity non-phase-matched third- and second-harmonic generation (THG and SHG), as well as multi-wavelength parametric mixing processes. Quite recently, these effects were observed [6] in two host-ceramics Sc_2O_3 and Lu_2O_3 with ordered structure for Ln^{3+} lasants (Table 1). The goal of this work was the observation of all possible nonlinear-laser effects related to the $\chi^{(3)}$- and $\chi^{(2)}$-nonlinearities in titled ceramics $Ba(Mg,Zr,Ta)O_3$ ("Lumicera type-Z") under one-micrometer picosecond laser pumping. For the purpose of clarity about current research on nonlinear-laser interactions in widely transparent crystalline ceramics, in Table 1 are included also the known to us published results in this field.

2 Ceramic fabrication and its some properties High-purity $BaCO_3$, ZrO_2, $MgCO_3$, and Ta_2O_5 powders were mixed with distilled H_2O in a ball mill and yielded a mixture of $Ba(Mg,Zr,Ta)O_3$. After the mixture was dried

Table 1 Nonlinear-laser effects in ceramics on the base of cubic oxides.

ceramics	space group[a)]	Ln^{3+} lasant	nonlinear-laser effect	SRS generation	
				ω_{SRS}, cm^{-1} [b)]	g_{ssR}^{St1}, cm GW^{-1} [c)]
Sc_2O_3	T_h^7	Yb^{3+}	SRS, SHG, THG, self-FM(SRS)[d)]	≈419	≈0.72 [7]
Y_2O_3	T_h^7	Nd^{3+}, Yb^{3+}	SRS	≈378	≈0.4 [8]
$Y_3Al_5O_{12}$	O_h^{10}	Nd^{3+}, Er^{3+}, Yb^{3+}	SRS	≈370	≈0.1 [9]
$Ba(Mg,Zr,Ta)O_3$[e)]	O_h^5	[f)]	SRS, SHG, THG, self-FM(SRS)[d)]	≈735	≈0.18
Lu_2O_3	T_h^7	Nd^{3+}, Yb^{3+}	SRS, SHG, THG, self-FM(SRS)[d)]	≈392	≈0.3 [10]

[a)] Grains of the ceramics are randomly oriented nano- and micro-size single crystals.
[b)] ω_{SRS} is the energy of SRS-promoting vibration mode.
[c)] g_{ssR}^{St1} is the steady-state Raman gain coefficient for the first Stokes lasing under one-micrometer picosecond pumping radiation from $Nd^{3+}:Y_3Al_5O_{12}$ laser.
[d)] Self-FM(SRS), i.e. self-sum(difference) frequency multiwavelength parametric mixing of the arising SRS lasing and pumping radiation.
[e)] "Lumicera type-Z" ceramics in microcrystalline grains of which the B′ and B″ octahedral sites are randomly occupied by unlike-valence cations Mg^{2+}, Zr^{4+}, and Ta^{5+}, i.e. in this material is realized the second law of crystal-field disorder [11].
[f)] This ceramics is the attractive disordered host-materials for Ln^{3+} lasants (e.g. Nd^{3+}, Yb^{3+}, and TM laser active ions).

and calcined, the calcined compact was milled in a ball mill with distilled H_2O and an organic binder for several hours. The milled compact was dried and granulated, and it yielded ceramic material powder. The powder was melted at a pressure of 2000 kg cm^{-2}, and it yielded a disk-shaped ceramic green body with 35 mm diameter and several millimeters thickness. The green body was fired at a temperature higher than 1500 °C in an oxygen atmosphere whose O_2 concentration was higher than that of air. From the sintered body mirror-polished samples were fabricated in the form of bars (≈20 × 6 × 5 mm^3) with mirror-polished ends for nonlinear-laser experiments and ≈2 mm thick plates (with cross section 6 × 5 mm^2) polished to the 14th class of surface finish for an investigation of mechanical characteristics.

The microhardness of $Ba(Mg,Zr,Ta)O_3$ ceramics was estimated using the well-known relation $H = k(P/d^2)$ (see, e.g. [12]), where k is the coefficient dependent on the indenter shape (equal to 1.854 for our case) and d is the diagonal of the indentation. The experiment was made by the use a microhardness gauge (PMT-3 type) with a diamond Vickers indenter. Measurements showed that for the ceramics studied $H \approx 950$ kg mm^{-2}.

Some known physical properties of a fine-grained $Ba(Mg,Zr,Ta)O_3$ ceramics are given in Table 2.

3 Multiwavelength Raman-induced nonlinear lasing For the observation of all possible $\chi^{(3)}$- and $\chi^{(2)}$-nonlinear cascaded lasing in "cubic" $Ba(Mg,Zr,Ta)O_3$ ceramics with "disordered" O_h^5-structure in its wide optical transmission region we carried out single-pass (cavity-free) laser experiments with the use of $Nd^{3+}:Y_3Al_5O_{12}$ picosecond ($\tau_p \approx 100$ ps) radiation at $\lambda_f = 1.06415$ μm wavelength. The nearly Gaussian profile pumping beam is focused into the ceramic sample with a lens ($f = 250$ mm), resulting in a beam-waist diameter of about 160 μm. The spectral composition of its nonlinear lasing emission was dispersed with a grating monochromator (McPherson Model 270 in Czerny–Turner arrangement) and recorded by a spectrometric SCMA system equipped with two Hamamatsu linear image sensors Si-CCD(3923-10224Q) and InGaAs-CCD (G904-512D) providing sufficient spectral sensitivity from the UV to ≈1.7 μm (see inset in Fig. 4). In consequence of the more careful matching of an excitation scheme and new Si-CCD detector for UV and visible regions compared to preliminary SRS measurements with this ceramic [16], we significantly widened its anti-Stokes wing generation (Figs. 4a and b) and observed nonlinear-laser $\chi^{(3)}$- and $\chi^{(2)}$-emission, namely expected SHG, as well as THG and its UV-surrounding $\chi^{(3)}$-cascaded Stokes and anti-Stokes lasing components. For reliable registration of these weak nonlinear laser effects we significant decreased (by using corresponding filters and other experimental ruses) the unwanted (saturated) influence of strong one-micrometer pump radiation and intense Stokes and anti-Stokes bands emission on the Si-CCD sensor and thus significantly enhanced its effective sensitivity in the region of harmonic generation. The results of these measurements are shown in Figs. 4c and d. Whereas all observed $\chi^{(3)}$-nonlinear components, including in the UV part of the SRS spectrum, are sufficiently understandable, while the observed SHG needs to be investigated with great care. It should be noted here that very weak SHG could be associated also with induced $\chi^{(2)}$-nonlinearity (local mechanical stress) and with the resulting plasma in micro-interstices (pores). But, these possible reasons are not likely to take place in our case.

Under our steady-state (ss) pumping condition for $Ba(Mg,Zr,Ta)O_3$ ceramics $\tau_p \approx 100$ ps $\gg T_2 = (\pi \Delta\nu_R)^{-1} \approx 0.3$ ps (here, T_2 is the phonon dephasing time of SRS-promoting vibration transition and $\Delta\nu_R \approx 36$ cm^{-1} is the line width of the Raman shifted line related to this transition, see Fig. 5), we can also roughly estimate the steady-state Raman gain coefficient for its first-Stokes lasing component at $\lambda_{St1} = 1.1545$ μm wavelength. To accomplish this, we restored to sufficiently tested method based on the well-known ratio [17] $g_{ssR}^{St1} I_p^{thr} l_{SRS} \approx 30$ and comparative measurement of "threshold" pump intensity (I_p^{thr}) of the confidently detectable first-Stokes lasing signals for our ceramics at $\lambda_{St1} = 1.1545$ μm and for selected reference

Table 2 Some characteristics of Ba(Mg,Zr,Ta)O_3 ceramics ("Lumicera type-Z") [a].

characteristics	
space group	$O_h^5 - Fm\bar{3}m$ (No. 225)[b]
formula units per primitive cell	$Z^{Br} = 2$
site symmetry (SS) and coordination number (CN) of cations[c]	Ba^{2+}: SS $-\bar{4}3m$ (A – site), CN = 6 Mg^{2+}, Zr^{4+}, Ta^{5+}; SS $- m\bar{3}m$ (B′ and B″ sites), CN = 6
density, g cm^{-3}	≈7.5 [13]
chemical composition, %[d]	Ba –21.49; Mg –4.75; Zr –5.41; Ta –9.41; O –53.55
microhardness (Knoop scale), kg mm^{-2}	$H \approx 950$
optical transparency range, μm[e]	≈0.32 –≈6.5 [14]
refractive index [13]	$n = 2.143$ ($\lambda = 0.435$ μm); $n = 2.104$ ($\lambda = 0.541$ μm) (see also Fig. 3)
abbe number [13]	$\nu_d = 29.4$
nonlinearity	$\chi^{(3)}$ and $\chi^{(2)}$
phonon spectrum extension, cm^{-1}	≈840
energy of SRS-active mode, cm^{-1}	≈735
line width of Raman shifted lines related to SRS-promoting vibration mode, cm^{-1}	$\Delta\nu_R \approx 36$
steady-state Raman gain coefficient for "one-micrometer" first Stokes lasing, cm GW^{-1}	g_{ssR}^{St1}, ≈ 0.18
possible applications	optical components [13], laser Raman frequency converters, laser host-material

[a] Using the ordered–disordered transformation mechanism, by introduction of Zr^{4+} ions in the D_{3d}^3-perovskite type "ordered" Ba($Mg_{1/2}Ta_{2/3}$)O_3 compound (see Fig. 1a) was obtained the O_h^5-cubic "disordered" Ba(Mg,Zr.Ta)O_3 compound (Fig. 1b). This compound was a basis for "Lumicera Z-type" ceramics fabrication [15].
[b] Randomly oriented ceramic grains are micrometer-sized single crystals with O_h^5-cubic perovskite structure (see Fig. 1).
[c] The B′ and B″ octahedral sites randomly occupy by unlike-valency cations Mg^{2+}, Zr^{4+}, and Ta^{5+}.
[d] Obtained by using electron scanning microscope JSM-7401F equipped with a device for X-ray microanalysis. The measurement was carried out in the point marked by a square in Fig. 2. In the ceramics, small amounts of other impurities are also present (≈5.39%), among them silicon (perhaps Si^{4+}) as a required additive in a fabrication process.
[e] See Fig. 3.

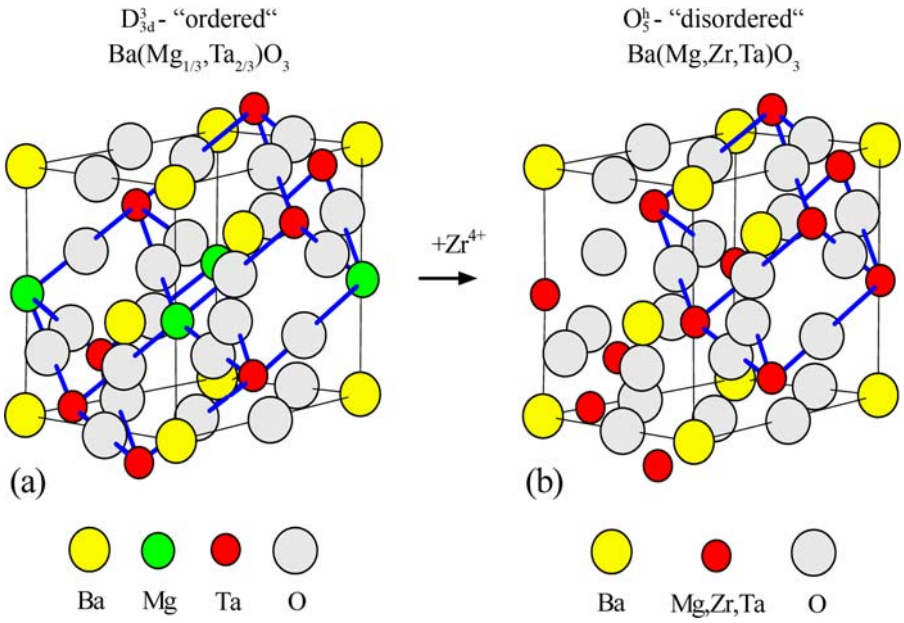

Figure 1 (online colour at: www.pss-a.com) Sections of the crystal structure of (a) "ordered" D_{3d}^3-perovskite type Ba($Mg_{1/2}Ta_{2/3}$)O_3 single crystal and (b) "disordered" O_h^5-cubic Ba(Mg,Zr,Ta)O_3 ceramics. The blue lines show the hexagonal and cubic structural units.

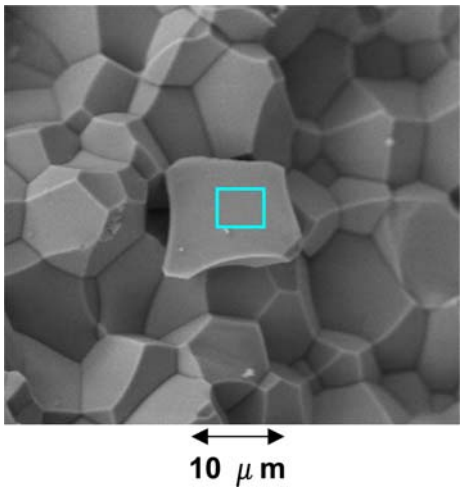

Figure 2 (online colour at: www.pss-a.com) Secondary electron image of a fracture of microcrystalline $Ba(Mg,Zr,Ta)O_3$ ceramics. See also text.

$PbWO_4$ crystal with the equal SRS-active length (l_{SRS}) at λ_{St1} = 1.1770 μm wavelength with the known value of the g_{ssR}^{St1} coefficient (≈3.1 cm GW^{-1} [18]). We found that the measured threshold for ceramics is seventeen times higher than that of the tungstate crystal. This results in a value of the Raman gain coefficient for $Ba(Mg,Zr,Ta)O_3$ ceramics not less than 0.18 cm GW^{-1}.

The factor-group analysis predicts for the O_h^5-primitive cell of our ceramics of $3NZ^{Br} = 30$ degrees of vibration freedom, which are described in accordance with (see, e.g. [19]) by the irreducible representations (at $\boldsymbol{k} = 0$): $\Gamma_{30} = \mathbf{A_{1g}} + \mathbf{E_g} + \mathbf{2F_{2g}} + F_{1g} + 5F_{1u} + F_{2u}$. Among them the three first species (marked by the bold) are the Raman-active modes; one F_{1u} corresponds to a triply degenerate acoustical mode, and the remaining four species of this type are the IR-active optical vibrations; F_{1g} and F_{2u} are the silent modes. The spontaneous Raman ($A_{1g} + E_g + 2F_{2g}$)-spectrum of $Ba(Mg,Zr,Ta)O_3$ ceramics studied (shown in Fig. 5) has recorded in roughly the same excitation geometry that we employ for mentioned above SRS measurements. As can be seen its general view is typical for Raman spectra of crystalline materials with disordered structure. In this stage of our investigation the detailed interpretation of this spectrum presents some problem due to lack of received X-ray data on the real distribution of unlike valency cations among octahedral B′ and B″ crystallographic sizes. While, on the basis numerous results of vibronic studies of the O_h^5-cubic perovskite-structure "disordered" crystalline materials (see, e.g. [20]), we tentative assumed that of intensive band at ≈735 cm^{-1} (which were related to the SRS-promoting vibration transition of the ceramics) may be due to the stretching B′–O–B″ vibration bonds.

Table 3 Spectral composition of $\chi^{(3)}$- and $\chi^{(2)}$-nonlinear laser generation in a $Ba(Mg,Zr,Ta)O_3$ ceramic with picosecond $Nd^{3+}:Y_3Al_5O_{12}$ laser pumping at fundamental wavelength λ_f = 1.06415 μm.

$\chi^{(3)}$- and $\chi^{(2)}$-nonlinear laser lines		
wavelength, μm[a)]	line[b)]	possible line attribution[c)]
0.3457	$ASt_1\lambda_{THG}$	$2\omega_f + \omega_{ASt1} = 3\omega_f + \omega_{SRS}$
0.3547	λ_{THG}	$3\omega_f$
0.3642	$St_1\lambda_{THG}$	$2\omega_f - \omega_{St1} = 3\omega_f - \omega_{SRS}$
0.3742	$St_2\lambda_{THG}$	$2\omega_f - \omega_{SRS} = 3\omega_f - 2\omega_{SRS}$
0.53207	λ_{SHG}	$2\omega_f$
0.7243	ASt_6	$\omega_f + 6\omega_{SRS}$
0.7650	ASt_5	$\omega_f + 5\omega_{SRS}$
0.8106	ASt_4	$\omega_f + 4\omega_{SRS}$
0.8619	ASt_3	$\omega_f + 3\omega_{SRS}$
0.9202	ASt_2	$\omega_f + 2\omega_{SRS}$
0.9870	ASt_1	$\omega_f + \omega_{SRS}$
1.06415	λ_f	ω_f
1.1545	St_1	$\omega_f - \omega_{SRS}$
1.2615	St_2	$\omega_f - 2\omega_{SRS}$

[a)] Measurement accuracy ±0.0003 μm.
[b)] For example, the condition notation of cascaded five-wave parametric process at 0.3457 μm wavelength is connected with two quanta of pumping (ω_f) and one quantum of first anti-Stokes generation ($\omega_f + \omega_{SRS}$), i.e. can be considered as anti-Stokes component of the third harmonic generation. It is also possible that other five-wave mixing cascades act.
[c)] ω_{SRS} ≈ 735 cm^{-1}.

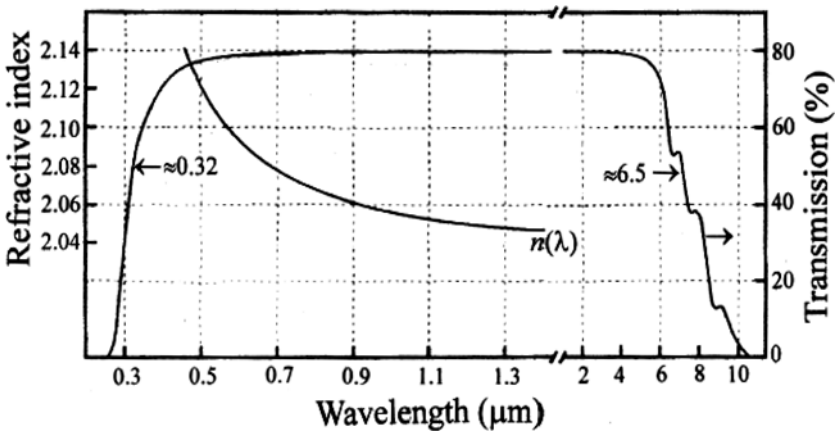

Figure 3 Wavelength dispersion of refractive index and transmission spectrum in the range from UV to the mid-IR with ≈1.5 mm (for UV–VIS–near-IR) and ≈0.6 mm thick polished plates without antireflection coating (see also [13]).

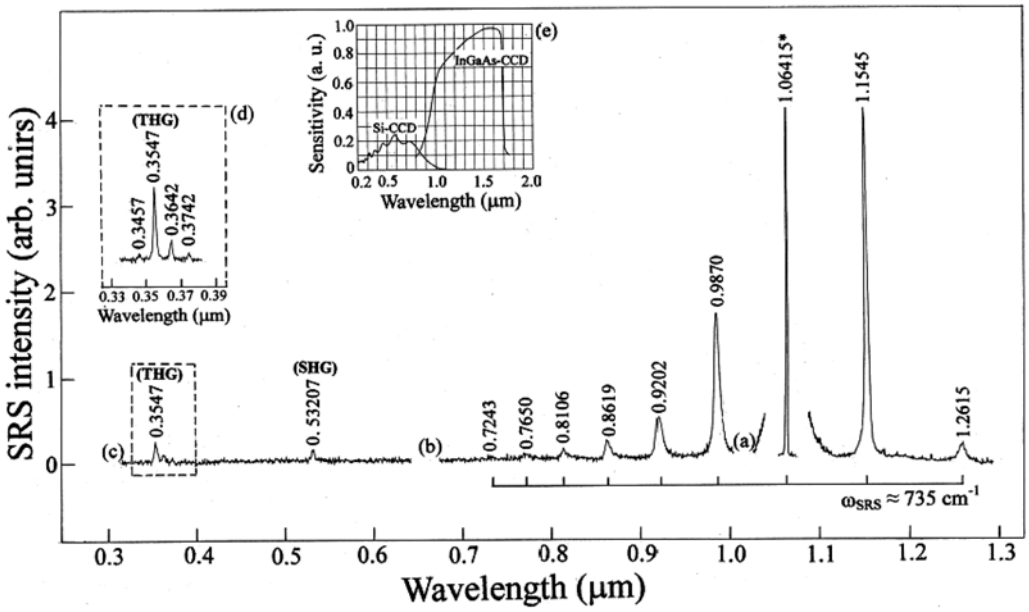

Figure 4 Fragments of $\chi^{(3)}$- and $\chi^{(2)}$-lasing spectrum of fine-grained Ba(Mg,Zr,Ta)O_3 ceramics with pumping at λ_f = 1.06415 μm wavelength of a $Nd^{3+}:Y_3Al_5O_{12}$ picosecond lasers and recorded by InGaAs-CCD sensor in the near-IR (fragment (a)) and by Si-CCD in the visible and UV regions (fragments (b), (c) and (d)), as well as spectral sensitivity (e) of the used Si- and InGaAs-CCD linear image sensors (data from Hamamatsu catalog). Parts (c) and (d) recorded under strong attenuation of one-micrometer pump and its near-IR intensive Stokes and anti-Stokes signals with different excitation levels. The wavelength of all lines is given in μm (the pump line is marked by an asterisk). Stokes and anti-Stokes components (see (a) and (b) fragments) related to SRS-promoting vibration mode $\omega_{SRS} \approx 735$ cm^{-1} are indicated by scale brackets.

4 Conclusions In the conducted SRS experiments with fine-grained ceramics based on Ba(Mg,Zr.Ta)O_3 oxide with "disordered" perovskite O_h^5-structure we have observed its high-order Raman-induced Stokes and anti-Stokes lasing, as well as SHG, THG, and cascaded parametric generation in the UV spectral region. All registered $\chi^{(3)}$ nonlinear-laser lines were identified and attributed to the SRS-promoting vibration mode $\omega_{SRS} \approx 735$ cm^{-1} of this novel highly transparent microcrystalline material. Its steady-state Raman gain coefficient $g_{ssR}^{St1} \approx 0.18$ cm GW^{-1} was estimated for the first Stokes generation under one-micrometer picosecond pumping. For fine-polished Ba(Mg,Zr,Ta)O_3 ceramics the microhardness ($H \approx 950$ kg mm^{-2}) was also measured using a diamond

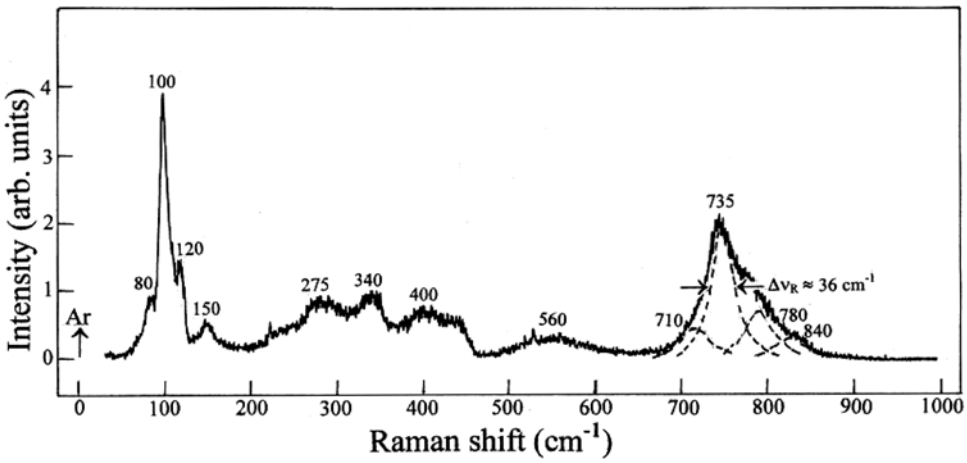

Figure 5 Room-temperature spontaneous Raman scattering spectrum of Ba(Mg,Zr,Ta)O_3 ceramic with "cubic" disordered structure that was recorded using a double-grating monochromator SG-100WD (Koken Kogyo) equipped with a photon counter C5410 (Hamamatsu). The arrow indicates the excitation line at the 0.488 μm wavelength of Ar-ion laser. The frequency of some Raman shifted lines is given in cm^{-1}.

Vickers indenter. There is no doubt that this "disordered" ceramic is also an attractive host-material for Ln^{3+} and TM lasants. It is probable that the SHG phenomenon related to the grain-boundary walls is the common property for highly transparent ceramics based on cubic oxides (see, e.g. [6]).

Acknowledgments The investigation reported here was greatly promoted by the cooperation within "Joint Open Laboratory for Laser Crystals and Precise Laser Systems" and supported in part by the Russian Foundation for Basic Research and the Program "Femtosecond optics and new optical materials" of the Russian Academy of Sciences, as well as the Technical University of Berlin and the 21st Century COE Program of the Ministry of Education, Culture, Sport, Science, and Technology of Japan. One of us (A.A.K.) is also grateful to the Alexander von Humboldt Foundation.

References

[1] A. A. Kaminskii, Laser Photon. Rev. **1**, 93 (2007).
[2] T. F. Soules, in: 3rd Laser Ceramic Symposium, CNRS, October 8–10, Paris, France, 2007, p. OG2.
[3] M. Tokurakawa, 3rd Laser Ceramic Symposium, CNRS, October 8–10, Paris, France, 2007, p. OL2.
[4] A. A. Kaminskii, M. Akchurin. R. Gainutdinov, K. Takaichi, A. Shirakawa, H. Yagi, T. Yanagitani, and K. Ueda, Crystallogr. Rep. **48**, 515 (2003).
L. Mezeiz and D. J. Gree, Int. J. Appl. Ceram. Technol. **3**, 166 (2006).
[5] N. Tanaka, Y. Kintaka, S. Kuretake, N. Wada, and Y. Sakabe, 2nd Laser Ceramic Symposium, Institute for Laser Science, November 10–11, Tokyo, Japan 2006, p. AS6.
[6] A. A. Kaminskii, H. Rhee, H. J. Eichler, K. Ueda, K. Takaichi, A. Shirakawa, M. Tokurakawa, J. Dong, H. Yagi, and T. Yanagitani, Laser Phys. Lett. **5**, 109 (2008).
[7] A. A. Kaminskii, S. N. Bagaev, K. Ueda, K. Takaichi, J. Lu, A. Shirakawa, H. Yagi, T. Yanagitani, H. J. Eichler, and H. Rhee, Laser Phys. Lett. **2**, 30 (2005).
[8] A. A. Kaminskii, K. Ueda, H. J. Eichler, S. N. Bagaev, K. Takaichi, J. Lu, H. Yagi, and T. Yanagitani, Laser Phys. Lett. **1**, 6 (2004).
[9] A. A. Kaminskii, H. J. Eichler, K. Ueda, S. N. Bagaev, G. M. A. Gad, J. Lu, T. Murai, H. Yagi, and T. Yanagitani, phys. stat. sol. (a) **181**, R19 (2000).
A. A. Kaminskii, H. J. Eichler, K. Ueda, S. N. Bagaev, G. M. A. Gad, J. Lu, T. Murai, H. Yagi, and T. Yanagitani, JETP Lett. **72**, 499 (2000).
[10] A. A. Kaminskii, S. N. Bagayev, H. J. Eichler, K. Takaichi, K. Ueda, A. Shirakawa, H. Yagi, T. Yanagitani, and H. Rhee, Laser Phys. Lett. **3**, 310 (2006).
[11] A. A. Kaminskii, phys. stat. sol. (a) **102**, 389 (1987).
[12] M. Sh. Akchurin, V. G. Galstyan, and V. R. Regel, Phys. Solid State **37**, 845 (1995).
M. Sh. Akchurin and V. R. Regel, Chem. Rev. **23**, 59 (1998).
[13] http://www.murata.com/ninfo/nr0572e.html.
[14] N. Tanaka, Ceramics **41**, 687 (2006), in Japanese.
[15] T. Nobuhiko, Japanese patent: JP200-4-075512,A.
[16] A. A. Kaminskii, N. Tanaka, H. J. Eichler, H. Rhee, K. Ueda, K. Takaichi, A. Shirakawa, M. Tokurakawa, Y. Kintaka, S. Kuretake, and Y. Sakabe, Laser Phys. Lett. **4**, 819 (2007).
[17] Y. R. Shen, The Principles of Nonlinear Optics (Wiley, New York, 1984).
[18] A. A. Kaminskii, C. L. McCray, H. R. Lee, S. W. Lee, D. A. Temple, T. H. Chyba, W. D. Marsh, J. C. Barnes, A. N. Annanenkov, V. D. Legun, H. J. Eichler, G. M. A. Gad, and K. Ueda, Opt. Commun. **183**, 277 (2000).
[19] D. L. Rousseau, R. P. Bauman, and S. P. S. Porto, J. Raman Spectrosc. **10**, 253 (1981).
[20] J. Zhou, Q. X. Su, K. M. Moulding, and D. J. Barber, J. Mater. Res. **12**, 596 (1997).
I. G. Siny, R. Tao, R. S. Katiyar, R. Guo, and A. S. Bhalla, J. Phys. Chem. Solids **59**, 181 (1998).
O. Svitelskiy, J. Toulouse, G. Yong, and Z. G. Ye, Phys. Rev. B **68**, 104107 (2003) and references therein.